

From iron curtain to green belt: Shift from heterotrophic to autotrophic nitrogen retention in the Elbe River over 35 years of passive restoration

Alexander Wachholz¹, James W Jawitz², Dietrich Borchardt¹

Formatiert: Deutsch (Deutschland)

¹Department of Aquatic Ecosystem Analysis and Management, Helmholtz-Centre for Environmental Research (UFZ), Magdeburg, Germany

²Soil and Water Sciences Department, University of Florida, Gainesville, FL, USA

Correspondence to: Alexander Wachholz (alexander.wachholz@uba.de)

Abstract. We investigate changes in in-stream nitrogen retention and metabolic processes in the River Elbe between 1978 and 2020. We analyzed multi-decadal time series data and developed a metabolic nitrogen demand model to explain trends in dissolved inorganic nitrogen (DIN) retention, gross primary production (GPP), and ecosystem respiration (ER) during a period of highly dynamic pollution pressures in the Elbe River (Central Europe). Our findings reveal a marked increase in summer DIN retention and a decrease in winter DIN retention, establishing a distinct seasonal pattern. We identified three periods in the Elbe's DIN retention dynamics: dominantly heterotrophic under high organic and inorganic pollution pressure (1980-1990), transition (1990-2003), and dominantly autotrophic with lower pollution (2003-2017). We link these changes to reduced industrial pollution, improved wastewater treatment, and a shift in the in-stream balance between heterotrophic and autotrophic processes. During the first period, high ER ~~and heterotrophic growth efficiency contributed~~ caused to elevated metabolic nitrogen demands, primarily driven by heterotrophic processes. As pollution from industrial and wastewater emissions decreased, GPP rates increased, and ER gradually declined, prompting a shift towards an autotrophic-dominated nitrogen retention regime. Our study indicates a tight coupling of nutrient reduction from external sources and dominant processes of natural attenuation in large rivers, which needs to be considered for projections of recovery trajectories toward sustainable water quality.

1 Introduction

Large river systems have been substantially impacted by anthropogenic pressures associated with economic development, including observed long-term trends of ecosystem degradation throughout much of the 20th century (Vörösmarty et al., 2015; Meybeck et al., 2018). However, ecosystem protection regulations promulgated in recent decades have supported the recovery of many river ecosystems (Minaudo et al., 2015; Westphal et al., 2019), including improvements in river metabolic regimes (Diamond et al., 2022a; Jarvie et al., 2022) and reduction of dissolved inorganic nitrogen loads (Wachholz et al., 2022). Much work has examined the terrestrial drivers of these multi-decadal trajectories of river ecosystems (Ehrhardt et al., 2019; Dupas et al., 2018; van Meter et al., 2017). However, little is known about the impact of those long-term changes on the in-stream processes. An important in-stream process that is susceptible to external pressures is in-stream retention of dissolved inorganic nitrogen (DIN), which plays a crucial role in watershed nitrogen (N) budgets. On the global scale, inland waters retain, often retaining over 30% of the inputs (Ritz and Fischer, 2019a; Rode et al., 2016; Wang et al., 2022) 60% of the annual terrestrial

[nitrogen input \(Schlesinger and Bernhardt, 2013\)](#). This important ecosystem function also helps protect downstream ecosystems from eutrophication (Bianchi et al., 2010) induced by highly reactive forms of nitrogen, such as nitrate and ammonium (Seitzinger et al., 2002). In-stream DIN retention is closely linked to other ecosystem functions, especially stream metabolism (Hall and Tank, 2003; Heffernan and Cohen, 2010³). Long-term changes of metabolism (Arroita et al., 2019), nitrogen loading (Ballard et al., 2019), and nitrogen composition (Wachholz et al., 2022) have been observed in rivers. Here, we are interested in associated long-term patterns of in-stream DIN retention.

[Here we use in-stream DIN retention as an overarching term for all processes that, temporarily or permanently, remove DIN from the water. These processes include assimilation by hetero- and autotrophic organisms, and denitrification.](#) In-stream DIN retention is performed by ~~algae~~-bacteria, ~~algae~~ and macrophytes in the water column and sediments (Deutsch et al., 2009; Middelburg and Nieuwenhuize, 2000), which either assimilate DIN into their biomass or use it for metabolic processes. The activity of these organisms is influenced by various environmental factors such as water temperature, residence time, and nutrient concentrations (Collos and Harrison, 2014^a; Rasmussen et al., 2011; Snell et al., 2019). While travel time (Bertuzzo et al., 2017) and water temperature (Sherman et al., 2016) are often assumed to be the primary controls of in-stream DIN retention, the composition of DIN can also play a significant role. For instance, $\text{NH}_4\text{-N}$ is favored over $\text{NO}_3\text{-N}$ by many algae and bacteria (Cejudo et al., 2020). If sufficient $\text{NH}_4\text{-N}$ is available, the DIN uptake by unicellular algae can increase by a factor of 2-16 (Collos and Harrison, 2014^b). Understanding of DIN retention should also consider the relative contributions of algae, bacteria, and macrophytes, which each have preferences for different DIN species (Bergbusch et al., 2021; Collos and Harrison, 2014), incorporate N at different stoichiometric ratios into their biomass (Diamond et al., 2022; Godwin and Cotner, 2018), and have different growth efficiencies (the ratio of consumed resources that are assimilated into biomass, e.g. del Giorgio, 1997).

While long-term trends in the drivers and correlates with in-stream DIN retention are relatively well known (e.g. Ballard et al., 2019; Wachholz et al., 2022, Diamond et al., 2022), their consequences on in-stream DIN retention itself are understudied. This leaves considerable uncertainty in long-term watershed N budgets, which are already uncertain due to hard-to-quantify phenomena, such as time lags (Lutz et al., 2022). Therefore, we propose the following research question: How do the magnitude and dominant processes of in-stream DIN retention change in response to long-term changes in DIN composition and river trophic regime? To answer this question, we studied the Elbe River from 1978 to 2017. During this period, the Elbe river underwent a significant transition: before 1990, most of its catchment lay beyond the iron curtain and experienced significant chemical pollution, especially from heavy fertilizer use due to the agro-industrial revolution in the [German Democratic Republic \(GDR\)](#) after the 1960s (Bauerkaemper, 2004). Furthermore, large amounts of untreated wastewater from urban and industrial areas further polluted the stream (Netzband et al., 2002). However, after the GDR's collapse in 1989, industrial facilities closed, and WWTPs were rapidly constructed in the 1990s following the German reunification in 1991, resulting in decreased emissions from these sources and improved water quality in the Elbe (Adams et al., 2001). Parts of the

Elbes remaining floodplain are now located within the European Green Belt with the aim to preserve its valuable functions for flood retention and biodiversity (Serra-Llobet et al., 2022).

70 Previous work suggests a shift from a heterotrophic ([primarily production / respiration < 1](#)) to an autotrophic-~~dominated~~
~~metabolic regime~~ system ([primarily production / respiration > 1](#); Doretto et al., 2020) following the reduction of riverine
biological oxygen demand in response to wastewater treatment improvements following the GDR collapse (Lehmann and
Rode, 2001). However, the concomitant changes in DIN retention during this period have not been examined.

75 Quantitative links between in-stream metabolism and nutrient retention have been described by many authors (Hall and Tank,
2003; Heffernan and Cohen, 2010; Kamjunke et al., 2021; Rode et al., 2016; Zhang et al., 2023). The N demand of [gross](#)
[primary production \(GPP\)](#) and [ecosystem respiration \(ER\)](#) in an ecosystem can be estimated, subject to assumptions about
growth efficiencies (the share of GPP/ER that leads to biomass growth), biomass C:N ratios, and photosynthetic/respiratory
quotients (O₂/C ratio during photosynthesis/respiration) (Hall and Tank, 2003^a). As both auto- and heterotrophic
microorganisms use DIN as their preferred N source (Rier and Stevenson, 2002) those assumptions allow us to link the
80 [dissolved oxygen \(DO\)](#) and the DIN balance of a river segment. Other processes, however, disturb this link by influencing
either DO or DIN but not both. Possible examples are other biologic processes such as nitrification (retains DO but does not
affect DIN budget directly) and denitrification (removes NO₃-N but does not consume DO). However, physicochemical effects
such as ad- or desorption of NH₄-N also influence the DIN budget of a river segment without affecting the DO budget (Triska
et al., 1994).

85 ~~We hypothesize a natural condition of strong coupling between metabolic processes and in-stream DIN retention (Heffernan
and Cohen, 2013), but we expect this coupling to be weakened during phases of high pollution (such as during the late phases
of the GDR before 1990), with re-emergent coupling as pollutant loads decrease (after 1990).~~ GPP in the Elbe is mostly caused
by phytoplankton (Hardenbicker et al., 2014), and [phytoplankton](#) ~~is~~ activity is closely linked to the in-stream N processes in
the Elbe in recent years (Ritz and Fischer, 2019; Kamjunke et al., 2021). In-stream denitrification is assumed to be of
~~minor~~ lesser importance ~~(10%)~~ in the Elbe, at least after the reunification (Ritz et al., 2017; Schulz et al., 2023). The strong
90 decrease in NH₄-N concentrations after 1990 (Adams et al., 2001^a) suggests that nitrification and sorption processes play a
minor role in the Elbe's DIN retention, [as less NH₄-N is available](#). Before 1990, in-stream oxygen concentrations were low
(Lehmann and Rode, 2001), and NH₄-N concentrations were high (Adams et al., 2001^b). We, therefore, expect that nitrification
and denitrification occurred at relatively higher rates with weaker coupling between DIN retention and metabolic processes.

95 [To summarize, we hypothesize a natural condition of strong coupling between metabolic processes and in-stream DIN
retention \(Heffernan and Cohen, 2010\) that we expect to be weakened during phases of high pollution \(such as during the late
phases of the GDR before 1990\), with re-emergent coupling as pollutant loads decrease \(after 1990\).](#)

To test our hypothesis, we quantified DIN retention using a two-station mass balance approach along [an 110](#) km, 8th-order
segment of Elbe with no noteworthy tributaries. Furthermore, we quantified changes in the trophic regime in the Elbe by

100 estimating gross primary production (GPP) and ecosystem respiration (ER) using the single-station hourly oxygen mass-
balance approach (Odum, 1956). We linked in-stream DIN retention to metabolic rates using stoichiometric constraints and
assessed the relative importance of autotrophic and heterotrophic processes.

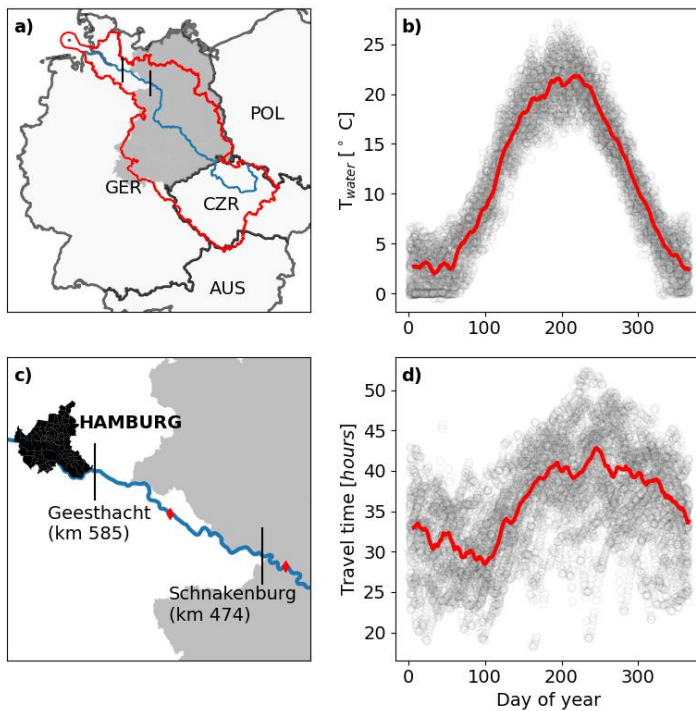
2 Data and methods

2.1 Overview

105 We used DIN and DO mass balances to assess the magnitude and responsible processes of in-stream DIN retention over 42
years from 1978 to 2020. We inversely modeled DO concentrations using a [Bayesian maximum likelihood estimation](#) method
to [estimate/quantify the in-stream](#) metabolic processes ([GPP, ER](#)) over time. We linked metabolism and in-stream DIN retention
using a simple model based on stoichiometric constraints and growth efficiencies.

2.2 Study site

110 We studied the last 111 km of a 1094 km 8th-order river (Elbe, Fig. 1a, b) between Schnakenburg (km 474) and Geesthacht
(km 585) which was a part of the Iron Curtain before 1990. [The German Elbe is free flowing, meaning that at least 474 km
upstream of the studied segment, no dams are present.](#) The studied segment has no noteworthy tributaries and is located 30 km
downstream of the last larger tributary (Havel), contributing between 10 and 20% of the Elbe discharge (Fig. S1). The annual
mean discharge at the downstream station Geesthacht (km 585) is $716 \text{ m}^3 \text{ s}^{-1}$ (IKSE, 2005). [Lateral groundwater discharge was
115 estimated to be \$<0.05 \text{ m}^3 \text{ s}^{-1} \text{ km}^{-1}\$ for the Elbe at stream km 450 \(Zill et al., 2023\), which corresponds to \$5.5 \text{ m}^3 \text{ s}^{-1}\$ for the entire
segment, less than 1% of the annual mean discharge, and was therefore not considered. We estimate the depth of the segment
to be between 2.8 and 4.5 m and the width between 270 and 450 m during flow conditions between the 5th and 95th percentile
\(see Section 2.5 for details\). PO₄-P concentrations oscillated between 0.2 and 0.3 mg l⁻¹ before 1990 and between 0 and 0.1
120 mg l⁻¹ afterward \(Wachholz et al., 2024\). The aquatic productive season occurs between April and October, as indicated by
\[increased Chlorophyll-a concentrations, and without macrophytes, primary production in the Elbe is assumed to be caused by
phytoplankton \\(Hardenbicker et al., 2018\\).\]\(#\)](#)



125 **Figure 1:** Location of the investigated river segment (a, c) in Europe. The blue line marks the Elbe main stream and the red outline represents the catchment. Black vertical lines mark the beginning and the end of the segment (sampling locations). Red diamonds in panel c indicate discharge gages. The former area of the German Democratic Republic (GDR) is represented by the grey shade. Intra-annual patterns of water temperature (b) and travel time (d). Circles show raw data, and red lines multi-year 7 day running means for each day of the year.

130 **2.3 Two-station mass-balance**

To quantify in-stream DIN retention; we use a two-station mass balance approach (e.g., Ritz and Fischer, 2019^a). [All samples were collected and analysed by the federal state authority of Lower Saxony. Nitrate samples were analysed with liquid ion-chromatography \(DIN EN ISO 10304-1\) and ammonium with flow analysis and spectrometric detection \(DIN EN ISO 11732\). It is not documented if and how the detection method changed over the monitored period. However, the time series exhibited](#)

135 [no obvious break points \(Fig. S2\)](#). The upstream site (Schnackenburg) is located at stream km [774474](#) and has weekly (1978-1991) and bi-weekly (1991-2021) water quality (NO₃-N and NH₄-N) time series available. Nitrite (NO₂-N) was not considered as, even in high nitrogen pollution periods, it made up between 1 and 3% of the DIN for both input and output (Fig. S23). [The upstream discharge gage \(Wittenberge\) is located 21 km upstream of the sampling site \(Fig. 1c\)](#). The downstream site (Geesthacht) at stream km [885585](#) has weekly NO₃-N and NH₄-N from 1980-1988, bi-weekly until 2006, and monthly afterward. A data gap from 1988-1993 [for the downstream site](#) was filled with data from another sampling site located at stream km 598 (Zollenspieker), as [both sites exhibit very similar nitrogen concentrations described in \(Wachholz et al. \(2022, their Figure S2\)](#). The [downstream](#) discharge gage (Neu Darchau) is located 50 km ~~down~~upstream of the sampling site used to estimate DIN load (station Geesthacht, [Fig. 1c](#)). However, the difference in catchment area between the sampling site and the gage is less than 3% (Wachholz et al., 2022). We consider this by assuming a 10 % error in discharge measurements in our uncertainty propagation, while a previous mass balance study (Ritz and Fischer, 2019) ~~assumed~~reported errors ≤ 5% in the Elbe, [according to personal communication with the state authorities responsible for the measurements. The same study also reported an error of 10 % for the laboratory quantification of nitrogen compounds according to the German standard procedures, which were also used in this study.](#)

2.3.1 WRTDS model

150 To reconcile differences in sampling dates between the upstream and downstream stations, daily loads of NO₃-N and NH₄-N were estimated using the weighted regression on time, discharge, and season (WRTDS) function of the R package EGRET (Hirsch et al., 2010). The WRTDS function uses a weighted regression approach to estimate daily loads and concentrations, accounting for non-linearity and non-stationarity in the relationships between the time, discharge, season, and concentrations over time. Measured and simulated daily concentrations showed very good agreement ($R^2 > 0.7$ and percent bias < 3, see Fig. 155 [S34](#)).

2.3.2 Retention metrics

Using the daily loads provided by the WRTDS function, we calculated in-stream DIN retention R_{obs} as

$$R_{obs} = L_{in} - L_{out} \quad (I)$$

160 where L is the DIN load [kg day⁻¹]. Uncertainty in R_{obs} , was computed based on Gaussian error propagation (Section S2). We then calculate the relative retention RR

$$RR_{obs} = \frac{R_{obs}}{L_{in}} \quad (II)$$

and the area weighted retention U [kg d⁻¹m²]

$$165 \quad U_{obs} = \frac{R_{obs}}{A} \quad (III)$$

where A [m^2] is the bottom area of the river segment (Stream Solute Workshop, 1990). We calculate R_{obs} , RR_{obs} , and U_{obs} for both DIN and $\text{NH}_4\text{-N}$. We corrected the L_{out} time series for travel time to align the inflow and outflow time series. The estimated travel times for the segment ranged from 19 and 52 hours (Fig. 1d), but since loads were only available as daily means, we evaluated corrections in increments of single days (Table S1-1), and we found that shifting L_{out} one day ahead of the L_{in} series yielded to the best results when a discharge mass balance was considered fit between the inflow and outflow time series.

2.4 Channel geometry estimations

Calculating area-weighted retention rates and inverse modeling of in-stream metabolism for a river segment requires knowledge of the surface area, water residence times, and channel depth. The methods to obtain these estimates are summarized below but are described in detail and validated in Section S1 and Fig. S5. We used discharge-based transfer functions to estimate the geometrical parameters at different water levels (e.g., Booker and Dunbar, 2008). We estimated travel time τ using a transfer function proposed by (Scharfe et al., 2009) for the German Elbe. For the channel area of the investigated segment, we established a transfer function based on discharge, which we parametrized with channel areas derived at different discharge conditions from Sentinel 2 images with a surface water detection algorithm (Normalized Difference Water Index). We employed a power law model for the channel depth based on data from Aberle et al. (2010).

Kommentiert [WA1]: This section was moved

2.5 Metabolism model estimations

The single station method for metabolism estimation in rivers with Bayesian inference uses dissolved oxygen (DO) data from a single monitoring station to estimate the rates of gross primary production (GPP) and ecosystem respiration (ER) in the river (e.g., Hall et al., 2016):

$$DO_{t+\Delta t} = DO_t + \frac{GPP}{PPFD_{24}} PPFD_t - ER \Delta t + \frac{k600 \left(\frac{Sc}{600}\right)^{\left(\frac{-1}{2}\right)} (DO_{max} - DO_t)}{z} \Delta t \quad (IV)$$

where $gppGPP$ and $erER$ are the daily rates [$\text{mmol m}^{-3} \text{d}^{-1}$] of the respective parameters, $PPFD_{24}$ is the photosynthetic photon flux density for the day and $PPFD$, per hour [$\mu\text{mol m}^{-3} \text{d}^{-1}$], $k600$ is the gas exchange coefficient rate [m d^{-1}], Sc is the dimensionless Schmidt number for oxygen (Wanninkhof, 1992) which is calculated based on water temperature, DO_t and DO_{max} are the actual and maximum (at 100% saturation) DO concentrations [$\mu\text{mol l}^{-1}$], and z is the channel depth [m]. The implementation of the Bayesian inference model to solve Eq. IV can be found in Section S4.

2.6 Data preparation and metabolism estimation

Implementation of Eq. IV requires hourly estimates of $PPFD$, DO , DO_{max} , z , and Sc . We interpolated diurnal DO concentrations by fitting sine functions to a time series of daily mean, minimum, and maximum values from 1978 to 2017, as described in

195 Section S3. Simulated DO concentrations were validated with two years of hourly measured values showing characteristics of
a good fit ($R^2=0.96$, $RMSE=0.42 \text{ mg l}^{-1}$). We estimated hourly solar radiation (as *PPFD*) based on the method proposed by
Duffie and Beckman (2013), which is implemented in the Python package *solarPy*. We calculated DO saturation based on the
method of Weiss (1970) using hourly air pressure data from the German weather service (DWD) station Seehausen (ID 4642)
and daily mean water temperature measured together with the DO data. We estimated $k600$ for the segment with a hydraulic
200 equation from Raymond et al. (2012, their Equation 7 of Table 2; see Section S4 for details) and ~~we used~~ we used maximum
likelihood estimation (e.g., van de Bogert et al., 2007) to fit parameter distributions for *GPP* and *ER* for each day of the time
series. We used a limited memory Broyden–Fletcher–Goldfarb–Shanno algorithm, implemented in the Python package *Scipy*
(Virtanen et al., 2020; function `minimize(method='L-BFGS-B')`) to minimize the negative log-likelihood between the modeled
DO concentrations and the observed DO data (e.g., van de Bogert et al., 2007). We constrained daily *GPP* and *ER* estimates
205 to be between 0 and $(-) 50 [\text{g O}_2 \text{ m}^{-2} \text{ d}^{-1}]$ and use $(-)10 [\text{g O}_2 \text{ m}^{-2} \text{ d}^{-1}]$ as an initial estimate.
Especially the use of estimated $k600$ and the daily mean water temperature might introduce large uncertainties to our *GPP* and
ER estimations. To quantify these uncertainties, we estimated the daily standard deviations σ of $k600$ (based on the parameter
variability described in Raymond et al., 2012), the daily water temperature (based on hourly data which are available some
years), and DO_{max} (based on the propagation of the standard deviations from water temperature) for each day (see Section S4).
210 We performed 100 bootstrap iterations for each day, drawing errors from normal distributions $N(0, \sigma)$ for the parameters
 $k600$, DO_{max} , and daily water temperature. We reported the mean and standard deviations of the resulting *GPP* and *ER*
estimations. We assessed the goodness of fit for the *GPP* and *ER* estimations by simulating DO concentrations using the mean
daily *GPP* and *ER* rates and comparing those to observed DO concentrations, reporting daily R^2 and root mean square error
values (Fig. S10). We further assessed the effects of the uncertainty of $k600$, DO_{max} and daily water temperature on *GPP* and
215 *ER* estimated by performing a simplified one-factor-at-a-time sensitivity analysis for two exemplary years (see Fig. S11). The
model implementation in Python can be found at (github.com/alexiwach/MetabolismModelElbe). We also assessed the areal
extent of the metabolic signal and found it in line with the mass balance analysis (see Section S4).

To estimate the effects of using daily instead of hourly water temperature measurements, we calculated the mean diurnal
temperature variability from 24 years of hourly water temperature in the Elbe, which is $1.1 \text{ deg C} (+0.7)$. For typical *DO*, *T*,
220 and *p* conditions at the Elbe, this can lead to a deviation in DO_{sat} of a maximum of 5.4 % (see Fig. S5), which we neglect in
the following analysis.

2.7 Estimating the N demand of metabolic processes

The demand of N caused by *GPP* and *ER* can be estimated based on the respective organisms' growth efficiency (*GE*), the
photosynthetic- and respiratory quotient (*PQ*, *RQ*), and the C:N ratio of their biomass (e.g., (Hall and Tank, 2003a). *GE* [-]
225 describes the proportion of resources and energy that is captured by photosynthesis (GE_{AUTO}) or respiration (GE_{HET}) that is
incorporated into new biomass (del Giorgio et al., 1997; Hall and Tank, 2003b). *PQ* and *RQ* describe the ratio of O_2 produced/
consumed per CO_2 consumed/ produced (Berggren et al., 2012; Hall and Tank, 2003a). Those two concepts can be used to

Kommentiert [WA2]: This section was rewritten according to the reviewers comments

assess how much C is incorporated into biomass for any given GPP and ER rate. Via the C:N ratio of the biomass ($C:N_{HET}$, $C:N_{AUT}$), the N demand can then be estimated. Since autotrophic and heterotrophic microbes prefer DIN to other forms of nitrogen (Rier and Stevenson, 2002) and DIN is always available at concentrations $> 1 \text{ mg l}^{-1}$, we interpret the N demand as DIN demand.

For autotrophic processes, we can formulate the following

$$U_{AUT}(t) = GPP(t) \frac{1}{PQ} \frac{GE_{AUT}}{C:N_{AUT}} \quad (V)$$

where U_{AUT} [$\text{mol m}^{-2} \text{ day}^{-1}$] is the DIN demand of the GPP rate [$\text{mol m}^{-3} \text{ day}^{-1}$], and PQ [$\text{mol C mol}^{-1} \text{ O}_2$], GE_{AUT} is the autotrophic growth efficiency [-], $C:N_{AUT}$ is the carbon to nitrogen ratio in the autotrophic biomass and z is the channel depth [m] used to convert volumetric GPP to areal retention rates. Similarly, we can formulate for heterotrophic processes

$$U_{HET}(t) = R_{het}(t) RQ \frac{GE_{HET}}{C:N_{HET}} \quad (VI)$$

however, it is well known that the measured ER is not only caused by heterotrophic bacteria, but also by autotrophs (e.g. Hall and Tank, 2003). A way to correct autotrophic respiration is to subtract the non-biomass-producing fraction of GPP from ER (Hall and Tank, 2003b).

$$R_{het}(t) = ER(t) - GE_{AUT} GPP(t) \quad (VII)$$

combining Eq. V, VI, and VII allows us to estimate the complete metabolic N demand U_{met} as follows

$$U_{met}(t) = \left(GPP(t) \frac{1}{PQ} \frac{GE_{AUTO}}{C:N_{AUTO}} + (ER(t) - GE_{AUTO} GPP(t)) RQ \frac{GE_{HET}}{C:N_{HET}} \right) z(t) \quad (VIII)$$

Calculating U_{met} based on GPP and ER rates, therefore, requires estimations of six parameters. For $C:N_{AUT}$, we use 7.3, which was reported for phytoplankton biomass in the Elbe. A recent study found that the C:N of phytoplankton biomass in the Elbe is around 7.3 (Kamjunke et al., 2021) and we applied the often used $PQ = 1$ [$\text{mol C mol}^{-1} \text{ O}_2$] and $GE_{AUTO} = 0.5$ (e.g., Hall and Tank, 2003b; Heffernan and Cohen, 2010; Rode et al., 2016). It is well known that the parameters $C:N_{HET}$, GE_{HET} , and RQ show strong variability across ecosystems (Godwin and Cotner, 2018; del Giorgio and Cole, 1998; Berggren et al., 2012). Since they all affect U_{met} , we evaluated three parameter combinations that would lead to low, intermediate, and high U_{met} values (Table 1).

Formatiert: Schriftart: Kursiv

Table 1: Parameter combinations for the estimation of the metabolic nitrogen demand. $C:N_{HET}$ is the carbon to nitrogen ratio of heterotrophic organisms, GE_{HET} is the heterotrophic growth efficiency [-] and RQ is the respiratory quotient [mol O₂ mol⁻¹ C].

Parameter combination	$C:N_{HET}$	GE_{HET}	RQ
Source	Godwin and Cotner (2018)	del Giorgio and Cole (1998)	Berggren et al (2012)
U_{METlow}	8	0.04	0.8
$U_{METmean}$	5	0.25	1.2
$U_{METhigh}$	4	0.6	1.6

We compared U_{met} estimated from each of these parameter combinations to U_{obs} based on the mass balance approach. U_{met} , as introduced here, only considers the nitrogen demand directly associated with assimilation related to primary production or respiration. Other processes, as e.g. denitrification, are not considered but discussed later.

We used $C:N_{HET} = 4.8$, the median ratio for aquatic bacteria presented by (Godwin and Cotner, 2018), and $RQ = 1.2$ (Berggren et al., 2012). GE_{HET} , on the other hand, is known to vary between 0.05 and 0.4 in freshwater ecosystems, with higher values under higher levels of organic pollution (del Giorgio et al., 1997). We fit Eq. VIII to U_{obs} data and only allow GE_{HET} to be variable. Although variability in $C:N_{HET}$ and RQ can be expected, we argue that the pollution gradient in GE_{HET} gives a strong indication for being variable over the time series. Furthermore, variability in $C:N_{HET}$ and RQ could be covered by variability in GE_{HET} , which we considered when interpreting the GE_{HET} parameter.

We fit Eq. VIII to the time series data for three periods, which corresponds to changes in the seasonality and magnitude of U_{obs} : 1980–1990, 1991–2002, 2003–2016 using the *curve_fit* method implemented in the python package SciPy (Virtanen et al., 2020) and constrain GE_{HET} between 0.05 and 1. To assess the variability of GE_{HET} towards highly influential data points, we perform the fitting for 100 randomly selected subsamples with 25 % of the original data. As the GE_{HET} values generated by this approach follow a normal distribution, we use their mean and standard deviation to describe their variability for uncertainty quantification.

As U_{obs} and U_{met} values have relatively high uncertainties during Regime 1 (Fig. 2; Fig. S9b), we chose a seasonality-based validation approach for the metabolic N demand model. For the U_{obs} and U_{met} time series, we compared the annual mean (μ), the day of the peak (ϕ), and the seasonality index (SI). We used a Monte Carlo approach to propagate the uncertainties of the fitted parameters GPP, ER, and GE_{HET} into the seasonality metrics. For each day where GPP, ER, and GE_{HET} estimates are available, we calculated daily minimum and maximum U_{met} values using the 90% confidence intervals determined from 100 random errors from the normal distributions defined by the daily mean and standard deviation of the respective parameter. We define minimum and maximum μ and SI values for each year based on these confidence intervals. For the day of the peak (ϕ), we analyze the time series of the 5th, 50th, and 95th percentile of U_{met} values for each year and report the earliest (lowest), mean, and latest (largest) ϕ . For U_{obs} , we repeat the same procedure, only that the basis for the error distribution is the Gaussian mass-balance error propagation described in Section 3.3.2.

Kommentiert [WA3]: This section was deleted as the method was adjusted

3. Results and Discussion

290

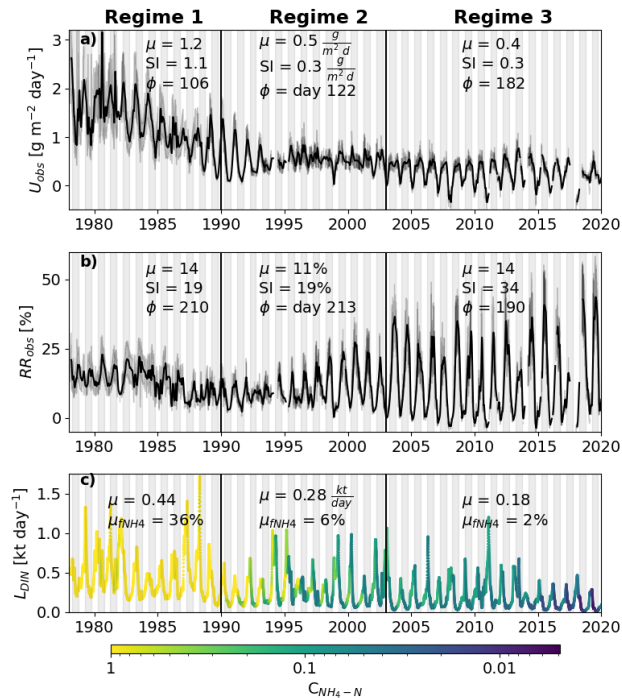


Figure 2: Area-weighted (U_{obs} , panel a) and relative dissolved inorganic nitrogen (DIN) retention rates (RR_{obs} , panel b) estimated using a two-station mass balance approach. The three black vertical lines correspond to the major changes in U : Regime 1 shows high mean (μ), strong seasonal amplitude (SI) and peaks during spring ($\Phi = \text{day } 106$). Regime 3 has a much lower μ and SI, while the day of the peak occurs during summer ($\Phi = 182$). Regime 2 represents the transition between both. The black lines represent a **30-day-30-day** moving average value, the shaded area around the black line shows raw values with a 90 % confidence interval. Panel c) shows the DIN load (L) received by the investigated segment of the Elbe. The color represents the corresponding ammonium concentration. μ_{NH_4} is the mean fraction of DIN that consists of ammonium. The white background **representrepresents** the colder six month of the year (October-April) and dark background the warmer six.

295

300

3.1 DIN retention

The highest U_{obs} values during the entire time series were observed during regime 1 (1978-1990), oscillating between 1 and 2 $\text{g m}^{-2} \text{d}^{-1}$ (Fig. 2a). Starting in mid of regime 1, U_{obs} decreased and oscillated mostly between 0 and 1 for the rest of the time series, with some negative values occurring during the winter in three years (2008, 2011, and 2018). During regime 1, U_{obs} peaked shortly before the [vegetation period-aquatic growing season](#) (days 106-122, [April-May](#)) and showed clear summer peaks (day 182, [July](#)) afterward. [The relative retention, however, showed a consistent summer peak during the entire time series \(days 190-220, July-August\) while the amplitude increased in regimes 2 and 3 \(19% to 34%\) \(Figure 2b\). Annual mean loads decreased throughout all three regimes from 0.44 to 0.18 \$\text{kt day}^{-1}\$ with a substantial decrease in annual minima around 1989 \(Figure 2c\). Likewise, the share of \$\text{NH}_4\text{-N}\$ from the DIN load declined from 36 to 6%. Concentrations of \$\text{NH}_4\text{-N}\$ did not reach values \$> 1 \text{ mg l}^{-1}\$ later in regime 2.](#)

[Peaks outside the warmer half of the year were not expected as water temperatures \(Sherman et al., 2016\) and residence times \(Bertuzzo et al., 2017\), considered the main drivers of in-stream DIN retention, are lower during this period. Furthermore, the amplitude of the oscillation \(\$SD\$ \) decreased after 1990 and remains constant for the rest of the time series.](#)

[The relative retention, however, showed a consistent summer peak during the entire time series \(days 190-220\) while the amplitude increased in regimes 2 and 3 \(19 to 34\) \(Figure 2b\).](#)

[Annual mean loads decreased throughout all three regimes from 0.44 to 0.18 \$\text{kt day}^{-1}\$ with a substantial decrease in annual minima around 1989 \(Figure 2c\). This coincided with the collapse of the GDR economy, which led to an immediate decrease in the inorganic and organic pollution of the River Elbe \(Adams et al., 2001b\). Likewise, the share of \$\text{NH}_4\text{-N}\$ from the DIN load declined from 36 to 6%. Concentrations of \$\text{NH}_4\text{-N}\$ did not reach values \$> 1 \text{ mg l}^{-1}\$ later in regime 2. This slower response could reflect the long-term improvements in wastewater treatment that followed the German reunification in 1990 \(IKSE, 2010\). This is further supported by the fact that \$\text{NH}_4\text{-N}\$ concentrations first decreased during the summer months, where dilution capabilities are lower, and the inputs from point sources play larger roles for the Elbes N regime \(Wachholz et al., 2022\).](#)

[Increases in area-weighted DIN retention of large rivers due to higher DIN pollution have already been reported by Kelly et al. \(2021\). They also remarked on changes in the drivers of \$U_{obs}\$, which reached high values even during the cold season during phases of high pollution, which agrees with our observations.](#)

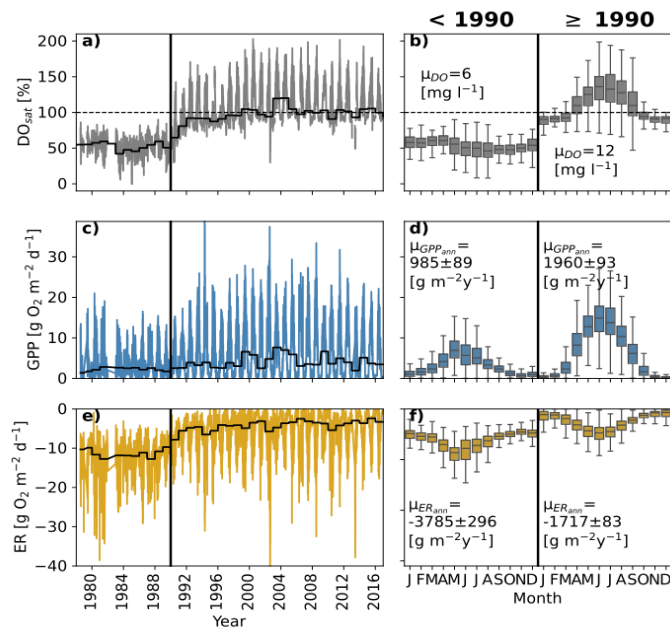
[During regime 3, \$U_{obs}\$ shows a stable pattern with peaks coinciding with high water temperatures and residence times \(Fig. 1b, e\). As neither temperature nor discharge exhibited noteworthy trends in seasonality in the Elbe during this period \(Markovic et al., 2013; Mudersbach et al., 2016\), we interpret this seasonality change as an indicator of a change in other driving processes, possibly in the responsible organisms. While the DIN input has a constant seasonal pattern, its magnitude and composition \(share of \$\text{NH}_4\text{-N}\$ \) changed remarkably throughout the time series \(Figure 2c\). As biota, such as algae, are known to form their](#)

Kommentiert [WA4]: This sentences have been moved.

assemblages according to environmental factors such as light, temperature, and nutrient availability (Snell et al., 2019), a biotic regime shift could have contributed to the U_{nlc} changes;

Kommentiert [WA5]: This section was moved and restructured in the discussion section

3.2 Metabolism



11Figure 3. Time series of daily dissolved oxygen saturation (DO_{sat} a), daily gross primary production estimates (GPP , c), and ecosystem respiration estimates (ER , e). The black lines show the annual median DO , GPP and ER values. Panels b, d, and f show the mean intra-annual monthly patterns (30-day moving means) for DO_{sat} , GPP , and ER , each before and after 1990. μ_{DO} represents the annual-mean values mean DO concentrations and μ_{GPPann}/μ_{ERann} the mean annual GPP to ER ratio.

Formatiert: Schriftfarbe: Schwarz, Englisch (Vereinigte Staaten), Tiefgestellt

3.2.1 DO_{sat} Oxygen saturation

The multi-decadal pattern of DO in the Elbe showed distinct behavior before and after 1990, coinciding with the German reunification and the collapse of the iron curtain (Figure 3a). Oxygen saturation before 1990 oscillated between 20 and 70%, but increased rapidly after 1990, reaching super-saturation for the first time in 1991. Before 1990 there was no clear intra-annual pattern (Figure 2b), but for the rest of the time series, DO_{sat} oscillated seasonally between ~80% and ~180%, peaking

around day 180, coinciding with the annual peaks of residence time, water temperature, and area-weighted DIN retention (Fig. 1b, c; Fig. 2a).

3.2.2 Gross primary production and ecosystem respiration

350 Similar to DO_{sat} , GPP showed a clear change around 1990 with low annual peaks (~~~10-15~~ $g\ O_2\ m^{-2}\ day^{-1}$) before and higher (~~~25-15-25~~ $g\ O_2\ m^{-2}\ day^{-1}$) in the following years (Fig 3c). Compared to DO_{sat} , the timing of the GPP peak stayed similar throughout the time series (~~~day-190~~ July), Fig 3d).

355 While the seasonal pattern of ER stayed similar (peaks in May, June, July) throughout the time series, annual ER rates were reduced to less than half after 1990 (Fig 3e, f). Most apparent are higher ER rates during the winter months before 1990. In contrast to GPP, ER rates started to change as early as 1987.

Considering annual mean net ecosystem productivity ($NEP = GPP - ER$), the investigated segment of the Elbe is a net-heterotrophic system before 1990 which means more O_2 is consumed than produced. High ER rates before 1990, led to a DO deficit of $\sim 2800\ g\ O_2\ m^{-2}\ year^{-1}$. After 1990 reduced ER and increased GPP rates turn the NEP of the segment and led to an oxygen surplus of $\sim 240\ g\ O_2\ m^{-2}\ year^{-1}$.

360

3.3 Linking Metabolism and DIN retention

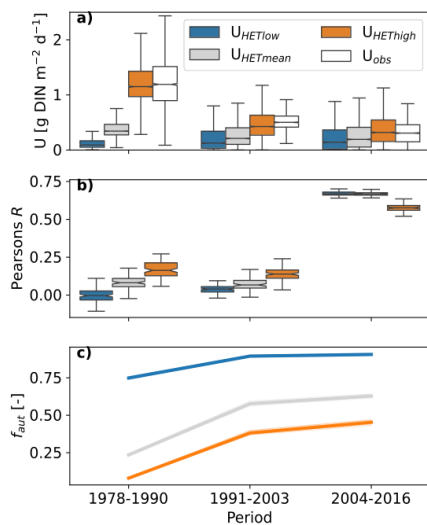


Figure 4. (a) Simulated and observed in-stream nitrogen retentions for three periods. The different colored boxplots represent the three parametrizations of heterotrophic nitrogen demands described in Table 1. U_{obs} represents retention rates based on the two-station mass balance described in Section 2.3. (b) Pearson correlation coefficients for the three parametrizations of heterotrophic nitrogen demands with U_{obs} . (c) Fraction of U caused by autotrophic nitrogen demand (f_{aut}) for the three parametrizations of heterotrophic nitrogen demands.

The different parametrizations of heterotrophic nitrogen demand show diverging performances over the three investigated periods which correspond to the three regimes of U_{obs} distinguished in Figure 2. Between 1978 and 2003, only the parameterization $U_{HEThigh}$ led to a similar distribution of U than observed (Figure 4a). During the last period (2004-2016), all parameter combinations led to U distributions that were similar to the observed. Pearsons R reveals poor correlation between simulated and observed U values before 2003, with the best results shown by the $U_{HEThigh}$ parameterization (Figure 4b). This changes for the period 2004-2016, where overall better R values were achieved, and the best results resulted from the parameterizations U_{HETlow} and $U_{HETmean}$. The share of autotrophic nitrogen demand on total metabolic nitrogen demand f_{aut} increased for all three parameterizations (Figure 4c). The highest f_{aut} values come from the parameterization with low heterotrophic nitrogen demand (U_{HETlow}) and vice versa.

Despite its conceptual nature, the metabolic N demand model showed promising results (Figure 4a-d). The confidence intervals of most seasonality metrics overlap between simulated and observed for almost the entire time series. The model consistently underestimated the observed annual mean (μ), but the overall tendency of decreasing values is well captured. The observed

385 amplitude metric SI is well predicted by the model during regimes 1 and 2, but is underpredicted during regime 3. This could be caused by the negative U_{obs} values, which cannot be captured by the model as all terms in Eq. VIII are positive. For the day of the peak (ϕ), the confidence intervals did not always overlap, but again, the general tendency of ϕ occurring during the cold season before 1990 and ϕ during the warm season (shaded area) after 1990 is well represented by the model (Fig 4d). The GE_{HET} parameter decreases between all three regimes with minimal variability inside the regimes (Fig 4a). In the first period (1980-1990), GE_{HET} was higher than previously reported values (≤ 0.4 from del Giorgio et al., 1997). It has to be acknowledged that variability of the terms $C:N_{HET}$ and RQ of Eq. VIII could also contribute to the fits. After 2003, GE_{HET} was reduced to the minimum allowed value of 0.05. This reduction fits overall well with the ammonium concentrations in the Elbe (Fig 2c), which were still relatively high (mean of 0.4 mg l^{-1} between 1990 and 2002) before they reached present low levels (mean of $< 0.06 \text{ mg l}^{-1}$). The R^2 comparing U_{obs} and U_{met} values is generally low during Regimes 1 and 2, reaching -0.7 in 2003-2017.

390 Fitting the metabolic N demand model allowed us to differentiate which share of in-stream DIN retention is caused by auto- (U_{AUT}) and heterotrophs (U_{HET}). U_{AUT} and U_{HET} show a clear trend over the investigated time period (Fig 5). During the 1980s, almost all metabolic N demand came from U_{HET} (84%), and only during summer/ fall did significant shares of U_{AUT} become visible. This relates well to observations of the low GPP rates before 1990 (Fig 3c, d), which should have translated into little U_{AUT} because little N is needed to support the low GPP rates. Before 1990, ER and GE_{HET} were very high, leading to an overall high metabolic N demand consistent with high U_{obs} values (e.g., Fig 4b). From 1990 until 2003, U_{HET} was still dominant for most of the year (66% of U_{met}), with summer peaks in U_{AUT} . After 1997, the seasonality of U_{HET} and U_{AUT} aligned. After 2003, U_{AUT} comprised most of U_{met} (64%). The river segment, however, remained net heterotrophic (annual mean ER $>$ GPP, Fig 3 d, f), but according to our results, little of that heterotrophic activity results in the assimilation of DIN into biomass ($GE_{HET} = 0.05$, Fig 3d). However, the low GE_{HET} value cannot be exclusively interpreted as a sign of low heterotrophic growth efficiency, as an increase in the heterotrophic C:N ratio (biomass with less N per C) could have the same effect on Eq. VIII. To facilitate the observed decrease in U , the C:N ratio of the heterotrophic biomass must have reached 50, while usually values in the range of 1 to 20 are being discussed (Godwin and Cotner, 2018). However, a combined increase in biomass C:N ratio and decreased growth efficiency seems plausible. This would not affect our interpretation as both the increased C:N ratio and decreased growth efficiencies represent a limited N demand of in-stream heterotrophic activity.

400 The model validation based on seasonality metrics suggested good model performance. Robust R^2 values were found only for the last period (2003-2017). While the seasonality-based validation considers the uncertainty in U_{met} and U_{obs} and compares the seasonal patterns, the R^2 compares actual U values. Considering our hypothesis, we interpret this as follows: While the seasonal patterns were consistently well represented by the U_{met} model, the R^2 reflects the strength of the coupling between the metabolic processes and the in-stream DIN retention. This only happened after ER developed a pattern following GPP (Fig. 3e). As the seasonal patterns of ER and GPP are well aligned during the period of high R^2 (Fig. 3d, f), we conclude they are now controlled by the same processes, (residence time and temperature/ light). ER is often higher during phases of higher

organic pollution loads (Arroita et al., 2019; Jarvie et al., 2022) as it is supported by organic substances from sewage. We speculate that the ER during regime 3 depended more on autochthonous organic matter production from phytoplankton.

Kommentiert [WA6]: This section was moved to the discussion and rewritten according to the adjusted metabolic n demand estimation

In summary, we explain the trends in U as follows: During regime 1 (1978–1990), the Elbe received high loads of particulate, organic, and inorganic pollution, which resulted in high ER and low GPP values. High ER and GE_{HET} values led to high metabolic N demand with a stochastic seasonal pattern driven by the ER mostly. High nitrification and possibly denitrification rates led to a weaker coupling of metabolic processes and U , which was still evident when seasonal patterns were used for validation. After the rapid decrease in industrial pollution around 1990, GPP rates increased swiftly while ER decreased gradually in response to improvements in wastewater treatment. This led to a transition from a heterotrophic to an autotrophic dominated DIN retention regime. Summer U increases fast while winter U decreases slowly, which leads to a reduced seasonal amplitude of U . Further improvements in wastewater treatment gradually remove the support for high ER rates, which become more dependent on the autochthonous organic material, leading to coinciding peaks of ER and GPP we see during regime 3. These coinciding peaks propagate into high U values during summer and low during winter, which we observe for the rest of the time series. A strong coupling emerges as the processes that decouple metabolism and DIN retention lose importance (nitrification, denitrification).

Kommentiert [WA7]: The content of this section was moved in to the discussion section

4. Discussion

4.1 DIN Retention

We classified observed in-stream nitrogen retention U_{obs} in three regimes: Regime 1 had the highest retention, a pronounced seasonal amplitude and peaked shortly before the beginning of the aquatic vegetation period, during the colder half of the year (Fig. 2a). Peaks outside the warmer half of the year were not expected as water temperature (Sherman et al., 2016) and residence time (Bertuzzo et al., 2017), considered the main drivers of in-stream DIN retention, are lower during this period. During regime 2, U_{obs} gradually decreased, reduced its amplitude, and shifted its annual peak into summer, where it remained in regime 3. Higher DIN retention rates during phases of higher DIN pollution, as observed in regime 1, have already been reported by Kelly et al. (2021). They also remarked on changes in the drivers of U_{obs} , which reached high values even during the cold season during phases of high pollution, which agrees with our observations. We interpret regime 2 as a transition period, corresponding to the long-term improvements in wastewater treatment that followed the German reunification in 1990 and took multiple years (IKSE, 2010). During this period NH_4 -N concentrations started to decrease during summer first, indicating changes in point source inputs (Wachholz et al., 2022). During regime 3, U_{obs} shows a stable pattern with peaks coinciding with high water temperatures and residence times (Fig. 1b, c).

As neither temperature nor discharge exhibited noteworthy trends in seasonality in the Elbe during the studied period (Markovic et al., 2013; Mudersbach et al., 2016), we interpret this seasonality change as an indicator of a change in other

450 driving processes, most likely in the abundance and metabolic activity of the responsible organisms. While the DIN input has a constant seasonal pattern, its magnitude and composition (share of $\text{NH}_4\text{-N}$) changed remarkably throughout the time series (Figure 2c). As biota, such as algae, are known to form their assemblages according to environmental factors such as light, temperature, and nutrient availability (Snell et al., 2019), a biotic regime shift could have contributed to the U_{obs} changes.

Kommentiert [WA8]: This section was just moved from the former results and discussion section

4.2 Metabolism

4.2.1 Dissolved Oxygen

455 Analyses of the oxygen saturation in the investigated segment of the Elbe revealed a constant saturation deficit, which was replaced by strong seasonal pattern with pronounced super-saturation during summer (Fig. 3a) after 1990. It is understood that the oxygen budget of the Elbe after 1990 is controlled by primary production, which rapidly increased after 1990 (Lehmann and Rode, 2001; Petersen and Callies, 2002). The absence of super-saturation before 1990 could be related to high concentrations of suspended solids, which are known to limit GPP in rivers (Trentman et al., 2022) and which were observed to decrease in the Elbe following the improvements in wastewater treatment after 1990 (Hillebrand et al., 2018). However, toxic effects from industrial waste also seem plausible, as concentrations for many organic and inorganic pollutants rapidly decreased around 1990 (Adams et al., 2001). However, a lack of primary production would not explain the significant saturation deficit of DO before 1990. From a mass balance perspective, only high rates of ER could have caused that phenomenon.

465 Further assessment of this requires the estimation of Elbe's metabolic processes which we carried out with a maximum likelihood estimation.

Kommentiert [WA9]: This section was just moved from the former results and discussion section

4.2.2 Gross primary production and ecosystem respiration

470 GPP and ER estimations revealed an increase in GPP and a decrease in ER around 1990 (Fig. 3c, d). While the GPP increase was sudden and mostly affected summer peaks, ER started to decrease in the late 1980s and also shows drastically reduced rates during the winter months. Compared to DO_{sat} , the timing of the GPP peak stayed similar throughout the time series (~ day 190 (July), Fig 3d), which suggests constant drivers but some limitation before 1990. It is well known that light and flow regimes control the metabolism of rivers (Bernhardt et al., 2022), so the peak during high temperature and residence times is to be expected and suggests another limiting factor before 1990 (e.g., high light attenuation from substances or sediments delivered by WWTP effluents).

475 The higher rates of ER before 1990 could have been supported by high loads of organic pollutants from wastewater (Adams et al., 1996). Compared to the increase in GPP, the slower ER decrease could be explained by the gradual improvements in water treatment throughout the 1990s and early 2000s (Adams et al., 2001; Wachholz et al., 2022). However, it has to be

480 acknowledged that ER started to change before 1990. This could have been caused by an early onset of the industrial collapse
of the GDR, affecting some industrial wastewater emitters, or by improved wastewater treatment before the GDR collapse.
Another interesting observation is the high winter ER before 1990. One must consider the term 'ER' from Eq. IV contains all
processes that consume DO in the balance, including nitrification. $\text{NH}_4\text{-N}$ was present in high concentrations in the River Elbe
before 1990 (Figure 2c). It is well known that nitrification can significantly contribute to oxygen depletion (Powers et al.,
2017) and that nitrification rates during cold periods increase with $\text{NH}_4\text{-N}$ concentrations (Cavaliere and Baulch, 2019). This
485 correlates to our observation of high DIN retention rates outside the warmer half of the year, as nitrifying and denitrifying
organisms also have nitrogen demands.

490 It has to be acknowledged that the metabolic estimations presented here are based on a few speculative assumptions.
Nevertheless, the model showed over all good agreement with the observed DO data (Fig. S10). R^2 was generally the highest
during spring (>0.8) and lowest in winter (~ 0.6). R^2 performance was similar for the period before and after 1990. Considering
the root mean square error, all seasons in both periods show values between 0 and $2.5 \text{ mg O}_2 \text{ m}^{-2} \text{ d}^{-1}$, with the exception of
summer after 1990, where the mean root mean square error is around $7 \text{ mg O}_2 \text{ m}^{-2} \text{ d}^{-1}$. This is, however, the part of the year
with the highest GPP and ER values, and since the R^2 in this period and season is >0.7 , we still consider the models performance
well.

495 Our simple one-factor-at-a-time sensitivity analysis revealed that both GPP and ER are most susceptible to changes in k600
(Fig. S11). Since this parameter was also estimated from a hydraulic equation and could not be verified for the studied segment,
this introduces an unquantified uncertainty to our results. GPP, however, was affected very little by variability in K600
compared to ER, and as similar summer GPP rates were found in the Elbe in other studies (e.g. Kamjunke et al., 2021) we
500 assume the GPP values and long-term changes to have a high certainty. The absolute ER and k600 values for the Elbe could
not be independently verified. However, the reduction of ER rates due to wastewater treatment improvements seems plausible.
If we assume k600 to be solely driven by hydraulic factors, for which we found no indication of change, then an overall
decrease of ER could be a likely mechanistic explanation of the observed changes in DO.

505 4.3 Linking Metabolism and DIN retention

510 Despite its simple nature, the metabolic N demand model showed promising results in predicting mean DIN retention rates
(Figure 4a-c). Between 1979 and 1990, only the parametrization U_{METHigh} was able to mimic the distribution of observed DIN
retention rates correctly. Only after 2003 did the model gain noteworthy predictive capabilities for the observed daily DIN
retention rates ($R \geq 0.7$) for the parametrization U_{METLow} and U_{METmean} , with the parametrization U_{METHigh} performing worse (R
 ≈ 0.5). The overall observation of low model performance before 2003 can be interpreted as a weakened coupling between
metabolic processes and in-stream DIN retention. As we hypothesized, processes such as denitrification, $\text{NH}_4\text{-N}$ sorption, and

Kommentiert [WA10]: This sections consists of parts from the former results and discussion section which have been adjusted to the updated results

Kommentiert [WA11]: This sections have been added respective to the comments on the uncertainty of our method

515 nitrification can impact the DIN and oxygen balance differentially, weakening the link between both elemental cycles. While we have no independent information on the rates of denitrification, $\text{NH}_4\text{-N}$ sorption, and nitrification in the studied segment before 1990, we argue that the circumstances indicate that they likely were higher than after 2000. With little $\text{NH}_4\text{-N}$ present in the segment after the improvements in wastewater treatment, neither sorption nor nitrification could have occurred at high rates. Nitrification, on the other hand, is assumed to have been a major drain on the oxygen budget of the Elbe before reunification (Wachholz et al., 2024). Denitrification is assumed to be a minor part of the Elbe's DIN retention in recent years (Schulz et al., 2023), but it is known that lower DO concentrations in eutrophic rivers, as were experienced in the Elbe before 1990, can promote denitrification (Rysgaard et al., 1994). The DIN retention after 2003 is likely largely due to assimilation by heterotrophic and autotrophic organisms and, therefore, closely linked to the metabolic processes, as indicated by the improved model performance in this period.

525 Our findings also have implications on how much of the metabolic nitrogen demand comes from the assimilation by autotrophic organisms. The U_{METhigh} parametrization, which is the only one able to explain the high DIN retention values before 1990 (Fig. 4a), predicts that more than 90% of DIN retention comes from heterotrophic nitrogen demands. Even if this parametrization is unrealistic and denitrification would have been a major part of the observed DIN retention, it seems likely that most DIN retention, at least before 1990, was caused by heterotrophic organisms. On the other hand, after 2003, the U_{METlow} and U_{METmean} show the best performance and predict that between 50% and 80% of the observed DIN retention was caused by autotrophic organisms. We interpret this as a shift between an in-stream DIN retention regime dominated by heterotrophic activity to one dominated by autotrophic activity.

535 As in-stream processes are greatly influenced by the hydro-climate of the river (e.g., Bernhardt et al., 2022) -and changes in its flow regime, as caused for example by dams (e.g. Aristi et al., 2014), these are competing drivers for the observed changes. At least as of 2013, no systematic trends in the Elbe's flow regime had been documented (Mudersbach et al., 2016). The Elbe's water temperature is rising (~ 0.01 °C per year) in concert with rising air temperatures, and a phase shift towards an earlier warming of two weeks has been described (Markovic et al., 2013). Based on these findings however we find it unlikely that hydro-climatic changes caused there here described changes in in-stream processes.

540 Our results also highlight the importance of the parameters RO , GH_{HET} , and $C:N_{\text{HET}}$, which, within reasonable bounds, can change heterotrophic nitrogen demand by a factor 10 (Fig. 4a). Understanding and constraining the variability in these parameters is therefore paramount for a better understanding of carbon, oxygen and nitrogen cycles in rivers. In our simple analysis, we ignored variability in the parameters $C:N_{\text{AUT}}$, GE_{AUT} , and PO , which could explain the still improvable fits of the metabolic nitrogen demand model after 2003.

Kommentiert [WA12]: This section was present before in the results and discussion section, but was adjusted according to the reviewers comments

Kommentiert [WA13]: This section has been added as a result of a reviewers comment

Kommentiert [WA14]: This section has been added as a result of a reviewers comment

34.4 Ecological implications

Long-term changes in GPP and ER can have a multitude of ecological implications for the river segment itself or downstream ecosystems. For example, high ER and low GPP, as we observed in the Elbe before 1990, can lead to increased riverine CO₂ emissions (Attemeyer et al., 2021). Higher primary production in the Elbe after 1990 caused greater export of organic matter to the estuary during summer, which supports higher rates of estuarine ecosystem respiration, which in turn decreases DO concentrations (Amann et al., 2012) and which reduces available habitats for fish species over extended stretches of the tidal zones in the estuary (Mann, 1996).

The changed seasonality of DIN retention also likely had an impact on downstream ecosystems. Even though absolute retention rates before 1990 were higher (Fig. 2a), only 20-25 % of DIN was retained during summer (Fig. 2b), when algal blooms are most likely to occur. After the German reunification, the decreased DIN load (Fig. 2c) and increased in-stream retention led to less DIN being exported to the estuary during summer, decreasing the probability of DIN induced estuarine algal blooms (Anderson et al., 2008).

45. Conclusions

Our study provides valuable insights into the long-term effects of inorganic and organic pollution reduction and the tight coupling with the ecosystem functions of DIN retention and metabolism within large rivers. The shift from a heterotrophic-dominated to an autotrophic-dominated DIN retention regime and the associated changes in the seasonal patterns has implications for the carbon cycle and algal blooms in downstream ecosystems.

Our findings highlight the importance of considering different dimensions of integrative ecosystem functions (metabolism, DIN retention) when assessing long-term ecological changes in rivers, such as eutrophication. Dissolved oxygen concentration time series alone are sufficient to support our findings of a heterotrophic- to autotrophic to heterotrophic regime shift, but estimates of GPP, ER, and DIN retention were required to support a quantitative assessment of the magnitude and consequences of this shift. The discovery of decoupled responses of ER and GPP to improvements in water quality offers new insights on the time scales of aquatic ecosystem responses to changing external forcing and informs realistic estimates for the efficiency of nutrient management and the achievement of environmental objectives.

Competing interests

The contact author has declared that none of the authors has any competing interests.

Acknowledgments

AW was funded by the Helmholtz-International Research School "Trajectories towards Water Security" (TRACER, grand no. HIRS-0017).

Author contribution statement

Conceptualization: all Authors
Methodology: AW, JWJ
580 Data curation: AW
Formal analyses and investigation: AW, JWJ
Writing (original draft): AW
Writing (review and editing): AW, JWJ, DB
Supervision: JWJ, DB

585

Data & Code availability

Q, DIN, temperature and DO time series can be downloaded from the FGG Elbe webportal www.elbe-datenportal.de/FisFggElbe/.

The code for the metabolism estimation can be found at github.com/alexiwach/MetabolismModelElbe. The cCode used for the mass balance analysis and figure creation is available from the author upon reasonable request.

590

References

Aberle, J., Nikora, V., Henning, M., Ettmer, B., Hentschel, B., 2010. Statistical characterization of bed roughness due to bed forms: A field study in the Elbe River at Aken, Germany. *Water Resources Research* 46. <https://doi.org/10.1029/2008WR007406>

595

Adams, M.S., Ballin, U., Gaumert, T., Hale, B.W., Kausch, H., Kruse, R., 2001. Monitoring selected indicators of ecological change in the Elbe River since the fall of the Iron Curtain. *Conservation* 28, 333–344. <https://doi.org/10.1017/S0376892901000364>

600

Amann, T., Weiss, A., Hartmann, J., 2012. Carbon dynamics in the freshwater part of the Elbe estuary, Germany: Implications of improving water quality. *Estuarine, Coastal and Shelf Science* 107, 112–121. <https://doi.org/10.1016/j.ecss.2012.05.012>

Formatiert: Deutsch (Deutschland)

Aristi, I., Arroita, M., Larrañaga, A., Ponsatí, L., Sabater, S., von Schiller, D., Elosegí, A., Acuña, V., 2014. Flow regulation by dams affects ecosystem metabolism in Mediterranean rivers. *Freshwater Biology* 59, 1816–1829. <https://doi.org/10.1111/fwb.12385>

Arroita, M., Elosegí, A., Hall Jr., R.O., 2019. Twenty years of daily metabolism show riverine recovery following sewage abatement. *Limnology and Oceanography* 64, S77–S92. <https://doi.org/10.1002/lno.11053>

Attermeyer, K., Casas-Ruiz, J.P., Fuss, T., Pastor, A., Cauvy-Fraunié, S., Sheath, D., Nydahl, A.C., Doretto, A., Portela, A.P., Doyle, B.C., Simov, N., Gutmann Roberts, C., Niedrist, G.H., Timoner, X., Evtimova, V., Barral-Fraga, L., Bašić, T., Audet, J., Deininger, A., Busst, G., Fenoglio, S., Catalán, N., de Eyto, E., Pilotto, F., Mor, J.-R., Monteiro, J., Fletcher, D., Noss, C., Colls, M., Nagler, M., Liu, L., Romero González-Quijano, C., Romero, F., Pansch, N., Ledesma, J.L.J., Pegg, J., Klaus, M., Freixa, A., Herrero Ortega, S., Mendoza-Lera, C., Bednařík, A., Fonvielle, J.A., Gilbert, P.J., Kenderov, L.A., Rulík, M., Bodmer, P., 2021. Carbon dioxide fluxes increase from day to night across European streams. *Commun Earth Environ* 2, 1–8. <https://doi.org/10.1038/s43247-021-00192-w>

Ballard, T.C., Sinha, E., Michalak, A.M., 2019. Long-Term Changes in Precipitation and Temperature Have Already Impacted Nitrogen Loading. *Environmental Science & Technology* 53, 5080–5090. <https://doi.org/10.1021/acs.est.8b06898>

Bauerkaemper, A., 2004. The Industrialization of Agriculture and its Consequences for the Natural Environment: An Inter-German Comparative Perspective. *Historical Social Research / Historische Sozialforschung* 29, 124–149.

Bergbusch, N.T., Hayes, N.M., Simpson, G.L., Leavitt, P.R., 2021. Unexpected shift from phytoplankton to periphyton in eutrophic streams due to wastewater influx. *Limnology and Oceanography* 66, 2745–2761. <https://doi.org/10.1002/lno.11786>

Berggren, M., Lapierre, J.-F., del Giorgio, P.A., 2012. Magnitude and regulation of bacterioplankton respiratory quotient across freshwater environmental gradients. *ISME J* 6, 984–993. <https://doi.org/10.1038/ismej.2011.157>

Bernhardt, E.S., Savoy, P., Vlah, M.J., Appling, A.P., Koenig, L.E., Hall, R.O., Arroita, M., Blaszcak, J.R., Carter, A.M., Cohen, M., Harvey, J.W., Heffernan, J.B., Helton, A.M., Hosen, J.D., Kirk, L., McDowell, W.H., Stanley, E.H., Yackulic, C.B., Grimm, N.B., 2022. Light and flow regimes regulate the metabolism of rivers. *Proceedings of the National Academy of Sciences* 119, e2121976119. <https://doi.org/10.1073/pnas.2121976119>

Bertuzzo, E., Helton, A.M., Hall, R.O., Battin, T.J., 2017. Scaling of dissolved organic carbon removal in river networks. *Advances in Water Resources* 110, 136–146. <https://doi.org/10.1016/j.advwatres.2017.10.009>

- Bianchi, T.S., DiMarco, S.F., Cowan, J.H., Hetland, R.D., Chapman, P., Day, J.W., Allison, M.A., 2010. The science of hypoxia in the Northern Gulf of Mexico: A review. *Science of The Total Environment* 408, 1471–1484.
640 <https://doi.org/10.1016/j.scitotenv.2009.11.047>
- Booker, D.J., Dunbar, M.J., 2008. Predicting river width, depth and velocity at ungauged sites in England and Wales using multilevel models. *Hydrological Processes* 22, 4049–4057. <https://doi.org/10.1002/hyp.7007>
- 645 Cavaliere, E., Baulch, H.M., 2019. Winter nitrification in ice-covered lakes. *PLOS ONE* 14, e0224864. <https://doi.org/10.1371/journal.pone.0224864>
- Cejudo, E., Taylor, W., Schiff, S., 2020. Epilithic algae from an urban river preferentially use ammonium over nitrate. undefined.
- 650
- Chapra, S.C., Di Toro, D.M., 1991. Delta Method For Estimating Primary Production, Respiration, And Reaeration In Streams. *Journal of Environmental Engineering* 117, 640–655. [https://doi.org/10.1061/\(ASCE\)0733-9372\(1991\)117:5\(640\)](https://doi.org/10.1061/(ASCE)0733-9372(1991)117:5(640))
- Collos, Y., Harrison, P.J., 2014a. Acclimation and toxicity of high ammonium concentrations to unicellular algae. *Marine Pollution Bulletin* 80, 8–23. <https://doi.org/10.1016/j.marpolbul.2014.01.006>
655
- del Giorgio, P.A., Cole, J.J., Cimbleris, A., 1997. Respiration rates in bacteria exceed phytoplankton production in unproductive aquatic systems. *Nature* 385, 148–151. <https://doi.org/10.1038/385148a0>
- 660 [del Giorgio, P.A., Cole, J.J., 1998. Bacterial Growth Efficiency in Natural Aquatic Systems. *Annual Review of Ecology and Systematics* 29, 503–541. https://doi.org/10.1146/annurev.ecolsys.29.1.503](https://doi.org/10.1146/annurev.ecolsys.29.1.503)
- Deutsch, B., Voss, M., Fischer, H., 2009. Nitrogen transformation processes in the Elbe River: Distinguishing between assimilation and denitrification by means of stable isotope ratios in nitrate. *Aquatic Sciences* 71, 228–237.
665 <https://doi.org/10.1007/s00027-009-9147-9>
- Diamond, J.S., Moatar, F., Cohen, M.J., Poirel, A., Martinet, C., Maire, A., Pinay, G., 2022a. Metabolic regime shifts and ecosystem state changes are decoupled in a large river. *Limnology & Oceanography* 67. <https://doi.org/10.1002/lno.11789>
- 670 [Doretto, A., Piano, E., Larson, C.E., 2020. The River Continuum Concept: lessons from the past and perspectives for the future. *Can. J. Fish. Aquat. Sci.* 77, 1853–1864. https://doi.org/10.1139/cjfas-2020-0039](https://doi.org/10.1139/cjfas-2020-0039)

Formatiert: Deutsch (Deutschland)

Duffie, J.A., Beckman, W.A., 2013. Solar Engineering of Thermal Processes. John Wiley & Sons.

675 Escoffier, N., Bensoussan, N., Vilmin, L., Flipo, N., Rocher, V., David, A., Métivier, F., Groleau, A., 2018. Estimating ecosystem metabolism from continuous multi-sensor measurements in the Seine River. *Environ Sci Pollut Res* 25, 23451–23467. <https://doi.org/10.1007/s11356-016-7096-0>

Formatiert: Deutsch (Deutschland)

680 Ehrhardt, S., Kumar, R., Fleckenstein, J.H., Attinger, S., Musolff, A., 2019. Trajectories of nitrate input and output in three nested catchments along a land use gradient. *Hydrology and Earth System Sciences* 23, 3503–3524. <https://doi.org/10.5194/hess-23-3503-2019>

Filoso, S., Palmer, M.A., 2011. Assessing stream restoration effectiveness at reducing nitrogen export to downstream waters. *Ecological Applications* 21, 1989–2006. <https://doi.org/10.1890/10-0854.1>

685

Gao, B., 1996. NDWI—A normalized difference water index for remote sensing of vegetation liquid water from space. *Remote Sensing of Environment* 58, 257–266. [https://doi.org/10.1016/S0034-4257\(96\)00067-3](https://doi.org/10.1016/S0034-4257(96)00067-3)

690 Godwin, C.M., Cotner, J.B., 2018. What intrinsic and extrinsic factors explain the stoichiometric diversity of aquatic heterotrophic bacteria? *ISME J* 12, 598–609. <https://doi.org/10.1038/ismej.2017.195>

Formatiert: Deutsch (Deutschland)

Guhr, H., Karrasch, B., Spott, D., 2000. Shifts in the Processes of Oxygen and Nutrient Balances in the River Elbe since the Transformation of the Economic Structure. *Acta Hydrochimica et Hydrobiologica* 28, 155–161. [https://doi.org/10.1002/1521-401x\(200003\)28:3<155::aid-ahch155>3.0.co;2-r](https://doi.org/10.1002/1521-401x(200003)28:3<155::aid-ahch155>3.0.co;2-r)

695

Hall, R.O., Tank, J.L., 2003. Ecosystem metabolism controls nitrogen uptake in streams in Grand Teton National Park, Wyoming. *Limnology and Oceanography* 48, 1120–1128. <https://doi.org/10.4319/lo.2003.48.3.1120>

700 Hall, R.O., Tank, J.L., Baker, M.A., Rosi-Marshall, E.J., Hotchkiss, E.R., 2016. Metabolism, Gas Exchange, and Carbon Spiraling in Rivers. *Ecosystems* 19, 73–86. <https://doi.org/10.1007/s10021-015-9918-1>

Hardenbicker, P., Rolinski, S., Weitere, M., Fischer, H., 2014. Contrasting long-term trends and shifts in phytoplankton dynamics in two large rivers. *International Review of Hydrobiology* 99, 287–299. <https://doi.org/10.1002/iroh.201301680>

Formatiert: Deutsch (Deutschland)

705 Heffernan, J.B., Cohen, M.J., 2010. Direct and indirect coupling of primary production and diel nitrate dynamics in a subtropical spring-fed river. *Limnology and Oceanography* 55, 677–688. <https://doi.org/10.4319/lo.2010.55.2.0677>

Hillebrand, G., Hardenbicker, P., Fischer, H., Otto, W., Vollmer, S., 2018. Dynamics of total suspended matter and phytoplankton loads in the river Elbe. *Journal of Soils and Sediments*. <https://doi.org/10.1007/s11368-018-1943-1>

710

Hirsch, R.M., Moyer, D.L., Archfield, S.A., 2010. Weighted Regressions on Time, Discharge, and Season (WRTDS), with an Application to Chesapeake Bay River Inputs I. *JAWRA Journal of the American Water Resources Association* 46, 857–880. <https://doi.org/10.1111/j.1752-1688.2010.00482.x>

715 IKSE, 2010. Abschlussbericht Aktionsprogramm Elbe 1996 – 2010. [Internationale Kommission zum Schutz der Elbe \(IKSE\)\(available at: www.ikse-mkol.org/fileadmin/media/user_upload/D/06_Publikationen/03_Aktionsprogramme%20und%20Bestandsaufnahmen/2010_IKSE-AP-Abschlussbericht.pdf.](https://www.ikse-mkol.org/fileadmin/media/user_upload/D/06_Publikationen/03_Aktionsprogramme%20und%20Bestandsaufnahmen/2010_IKSE-AP-Abschlussbericht.pdf)

Formatiert: Deutsch (Deutschland)

720 IKSE, 2005. †Die Elbe und ihr Einzugsgebiet: Ein geographisch-hydrologischer und wasserwirtschaftlicher Überblick‡. Internationale Kommission zum Schutz der Elbe (IKSE). (available at: <https://digital.bibliothek.uni-halle.de/pe/content/titleinfo/1485813>).

725 Jarvie, H.P., Macrae, M.L., Anderson, M., Celmer-Repin, D., Plach, J., King, S.M., 2022. River metabolic fingerprints and regimes reveal ecosystem responses to enhanced wastewater treatment. *Journal of Environmental Quality* 51, 811–825. <https://doi.org/10.1002/jeq2.20401>

730 Kamjunke, N., Beckers, L.-M., Herzsprung, P., von Tümpling, W., Lechtenfeld, O., Tittel, J., Risse-Buhl, U., Rode, M., Wachholz, A., Kallies, R., 2022. Lagrangian profiles of riverine autotrophy, organic matter transformation, and micropollutants at extreme drought. *Science of The Total Environment* 828, 154243.

Kamjunke, N., Rode, M., Baborowski, M., Kunz, J.V., Zehner, J., Borchardt, D., Weitere, M., 2021. High irradiation and low discharge promote the dominant role of phytoplankton in riverine nutrient dynamics. *Limnology and Oceanography* n/a. <https://doi.org/10.1002/lno.11778>

735

Kelly, M.C., Zeglin, L.H., Husic, A., Burgin, A.J., 2021. High Supply, High Demand: A Fertilizer Waste Release Impacts Nitrate Uptake and Metabolism in a Large River. *JGR Biogeosciences* 126. <https://doi.org/10.1029/2021JG006469>

Lehmann, A., Rode, M., 2001. Long-term behaviour and cross-correlation water quality analysis of the river Elbe, Germany.

740 [Water Research 35, 2153–2160. https://doi.org/10.1016/S0043-1354\(00\)00488-7](https://doi.org/10.1016/S0043-1354(00)00488-7)

Formatiert: Deutsch (Deutschland)

Lutz, S., Ebeling, P., Musolff, A., Nguyen, T., Sarrazin, F., Van Meter, K., Basu, N., Fleckenstein, J., Attinger, S., Kumar, R., 2022. Pulling the Rabbit out of the Hat: Unravelling Hidden Nitrogen Legacies in Catchment-Scale Water Quality Models. *Hydrological Processes* 36. <https://doi.org/10.1002/hyp.14682>

745

[Mann, R.H.K., 1996. Environmental requirements of European non-salmonid fish in rivers. *Hydrobiologia* 323, 223–235. https://doi.org/10.1007/BF00007848](https://doi.org/10.1007/BF00007848)

Formatiert: Deutsch (Deutschland)

Formatiert: Deutsch (Deutschland)

Formatiert: Deutsch (Deutschland)

Feldfunktion geändert

750 Markovic, D., Scharfenberger, U., Schmutz, S., Pletterbauer, F., Wolter, C., 2013. Variability and alterations of water temperatures across the Elbe and Danube River Basins. *Climatic Change* 119, 375–389. <https://doi.org/10.1007/s10584-013-0725-4>

Middelburg, J., Nieuwenhuize, J., 2000. Nitrogen uptake by heterotrophic bacteria and phytoplankton in the nitrate-rich Thames estuary. *Mar. Ecol. Prog. Ser.* 203, 13–21. <https://doi.org/10.3354/meps203013>

755

[Minaudo, C., Meybeck, M., Moatar, F., Gassama, N., Curie, F., 2015. Eutrophication mitigation in rivers: 30 Years of trends in spatial and seasonal patterns of biogeochemistry of the Loire River \(1980-2012\). *Biogeosciences* 12, 2549–2563. https://doi.org/10.5194/bg-12-2549-2015](https://doi.org/10.5194/bg-12-2549-2015)

760 Modi, P., Revel, M., Yamazaki, D., 2022. Multivariable Integrated Evaluation of Hydrodynamic Modeling: A Comparison of Performance Considering Different Baseline Topography Data. *Water Resources Research* 58. <https://doi.org/10.1029/2021WR031819>

765 Mudersbach, C., Bender, J., Netzel, F., 2016. An analysis of changes in flood quantiles at the gauge Neu Darchau (Elbe River) from 1875 to 2013. *Proc. IAHS* 373, 193–199. <https://doi.org/10.5194/piahs-373-193-2016>

Formatiert: Deutsch (Deutschland)

Netzband, A., Reincke, H., Bergemann, M., 2002. The river elbe. *Journal of Soils and Sediments* 2. <https://doi.org/10.1007/BF02988462>

770 Pathak, D., Hutchins, M., Brown, L.E., Loewenthal, M., Scarlett, P., Armstrong, L., Nicholls, D., Bowes, M., Edwards, F., Old, G., 2022. High-resolution water-quality and ecosystem-metabolism modeling in lowland rivers. *Limnology and Oceanography* 67, 1313–1327. <https://doi.org/10.1002/lno.12079>

Petersen, W., Callies, U., 2002. Assessment of Primary Production by Statistical Analysis of Water-quality Data. Acta hydrochimica et hydrobiologica 30, 34–40. [https://doi.org/10.1002/1521-401X\(200207\)30:1<34::AID-AHEH34>3.0.CO;2-M](https://doi.org/10.1002/1521-401X(200207)30:1<34::AID-AHEH34>3.0.CO;2-M)

Powers, S.M., Baulch, H.M., Hampton, S.E., Labou, S.G., Lottig, N.R., Stanley, E.H., 2017. Nitrification contributes to winter oxygen depletion in seasonally frozen forested lakes. Biogeochemistry 136, 119–129. <https://doi.org/10.1007/s10533-017-0382-1>

Rasmussen, J.J., Baattrup-Pedersen, A., Riis, T., Friberg, N., 2011. Stream ecosystem properties and processes along a temperature gradient. Aquat Ecol 45, 231–242. <https://doi.org/10.1007/s10452-010-9349-1>

Raymond, P.A., Zappa, C.J., Butman, D., Bott, T.L., Potter, J., Mulholland, P., Laursen, A.E., McDowell, W.H., Newbold, D., 2012. Scaling the gas transfer velocity and hydraulic geometry in streams and small rivers. Limnology and Oceanography: Fluids and Environments 2, 41–53. <https://doi.org/10.1215/21573689-1597669>

Rier, S.T., Stevenson, R.J., 2002. Effects of light, dissolved organic carbon, and inorganic nutrients [2pt] on the relationship between algae and heterotrophic bacteria in stream periphyton. Hydrobiologia 489, 179–184. <https://doi.org/10.1023/A:1023284821485>

Ritz, S., Dähnke, K., Fischer, H., 2017. Open-channel measurement of denitrification in a large lowland river. Aquat Sci 80, 11. <https://doi.org/10.1007/s00027-017-0560-1>

Ritz, S., Fischer, H., 2019a. A Mass Balance of Nitrogen in a Large Lowland River (Elbe, Germany). Water 11, 2383. <https://doi.org/10.3390/w11112383>

Rode, M., Halbedel Née Angelstein, S., Anis, M.R., Borchardt, D., Weitere, M., 2016. Continuous In-Stream Assimilatory Nitrate Uptake from High-Frequency Sensor Measurements. Environ Sci Technol 50, 5685–5694. <https://doi.org/10.1021/acs.est.6b00943>

Rysgaard, S., Risgaard-Petersen, N., Niels Peter, S., Kim, J., Lars Peter, N., 1994. Oxygen regulation of nitrification and denitrification in sediments. Limnology and Oceanography 39, 1643–1652. <https://doi.org/10.4319/lo.1994.39.7.1643>

Salvatier, J., Wiecki, T.V., Fonnesbeck, C., 2016. Probabilistic programming in Python using PyMC3. PeerJ Comput. Sci. 2, e55. <https://doi.org/10.7717/peerj-cs.55>

Formatiert: Deutsch (Deutschland)

Formatiert: Deutsch (Deutschland)

Formatiert: Deutsch (Deutschland)

Formatiert: Deutsch (Deutschland)

Formatiert: Deutsch (Deutschland)

Savoy, P., Appling, A.P., Heffernan, J.B., Stets, E.G., Read, J.S., Harvey, J.W., Bernhardt, E.S., 2019. Metabolic rhythms in flowing waters: An approach for classifying river productivity regimes. *Limnology and Oceanography* 64, 1835–1851.

810 <https://doi.org/10.1002/lno.11154>

Scharfe, M., Callies, U., Blöcker, G., Petersen, W., Schroeder, F., 2009. A simple Lagrangian model to simulate temporal variability of algae in the Elbe River. *Ecological Modelling* 220, 2173–2186. <https://doi.org/10.1016/j.ecolmodel.2009.04.048>

815 [Schlesinger, W.H., Bernhardt, E.S., 2013. Inland Waters, in: Biogeochemistry. Elsevier, pp. 275–340. https://doi.org/10.1016/B978-0-12-385874-0.00008-X](https://doi.org/10.1016/B978-0-12-385874-0.00008-X)

[Schulz, G., van Beusekom, J.E.E., Jacob, J., Bold, S., Schöl, A., Ankele, M., Sanders, T., Dähnke, K., 2023. Low discharge intensifies nitrogen retention in rivers – A case study in the Elbe River. *Science of The Total Environment* 904, 166740.](https://doi.org/10.1016/j.scitotenv.2023.166740)

820 <https://doi.org/10.1016/j.scitotenv.2023.166740>

Seitzinger, S.P., Styles, R.V., Boyer, E.W., Alexander, R.B., Billen, G., Howarth, R.W., Mayer, B., Breemen, N.V., 2002. Nitrogen retention in rivers: Model development and application to watersheds in the northeastern U.S.A., in: *Biogeochemistry*. Springer, pp. 199–237. <https://doi.org/10.1023/A:1015745629794>

825

Serra-Llobet, A., Jähnig, S.C., Geist, J., Kondolf, G.M., Damm, C., Scholz, M., Lund, J., Opperman, J.J., Yarnell, S.M., Pawley, A., Shader, E., Cain, J., Zingraff-Hamed, A., Grantham, T.E., Eisenstein, W., Schmitt, R., 2022. Restoring Rivers and Floodplains for Habitat and Flood Risk Reduction: Experiences in Multi-Benefit Floodplain Management From California and Germany. *Frontiers in Environmental Science* 9. <https://doi.org/10.3389/fenvs.2021.778568>

830

Sherman, E., Moore, J.K., Primeau, F., Tanouye, D., 2016. Temperature influence on phytoplankton community growth rates. *Global Biogeochemical Cycles* 30, 550–559. <https://doi.org/10.1002/2015GB005272>

Snell, M.A., Barker, P.A., surridge, B.W.J., Benskin, C.H.M., Barber, N., Reaney, M., tych, W., Mindham, D., Large, A.R.G., Burke, S., Haygarth, M., 2019. Strong and recurring seasonality revealed within stream diatom assemblages. *Scientific Reports*

835 9. <https://doi.org/10.1038/s41598-018-37831-w>

[Speckhann, G.A., Kreibich, H., Merz, B., 2021. Inventory of dams in Germany. *Earth System Science Data* 13, 731–740. https://doi.org/10.5194/essd-13-731-2021](https://doi.org/10.5194/essd-13-731-2021)

Formatiert: Deutsch (Deutschland)

Formatiert: Deutsch (Deutschland)

Feldfunktion geändert

Formatiert: Deutsch (Deutschland)

Formatiert: Deutsch (Deutschland)

840 Trentman, M.T., Tank, J.L., Davis, R.T., Hanrahan, B.R., Mahl, U.H., Roley, S.S., 2022. Watershed-scale Land Use Change
Increases Ecosystem Metabolism in an Agricultural Stream. *Ecosystems* 25, 441–456. <https://doi.org/10.1007/s10021-021-00664-2>

Triska, F.J., Jackman, A.P., Duff, J.H., Avanzino, R.J., 1994. Ammonium sorption to channel and riparian sediments: A
845 transient storage pool for dissolved inorganic nitrogen. *Biogeochemistry* 26, 67–83. <https://doi.org/10.1007/BF02182880>

Tromboni, F., Hotchkiss, E.R., Schechner, A.E., Dodds, W.K., Poulson, S.R., Chandra, S., 2022. High rates of daytime river
metabolism are an underestimated component of carbon cycling. *Commun Earth Environ* 3, 270.
<https://doi.org/10.1038/s43247-022-00607-2>

850

[Van de Bogert, M.C., Carpenter, S.R., Cole, J.J., Pace, M.L., 2007. Assessing pelagic and benthic metabolism using free water
measurements. *Limnology and Oceanography: Methods* 5, 145–155. <https://doi.org/10.4319/lom.2007.5.145>](#)

Vannote, R.L., Minshall, G.W., Cummins, K.W., Sedell, J.R., Cushing, C.E., 1980. The River Continuum Concept. *Can. J.*
855 *Fish. Aquat. Sci.* 37, 130–137. <https://doi.org/10.1139/f80-017>

Virtanen, P., Gommers, R., Oliphant, T.E., Haberland, M., Reddy, T., Cournapeau, D., Burovski, E., Peterson, P., Weckesser,
W., Bright, J., van der Walt, S.J., Brett, M., Wilson, J., Millman, K.J., Mayorov, N., Nelson, A.R.J., Jones, E., Kern, R., Larson,
E., Carey, C.J., Polat, İ., Feng, Y., Moore, E.W., VanderPlas, J., Laxalde, D., Perktold, J., Cimman, R., Henriksen, I., Quintero,
860 E.A., Harris, C.R., Archibald, A.M., Ribeiro, A.H., Pedregosa, F., van Mulbregt, P., SciPy 1.0 Contributors, 2020. SciPy 1.0:
Fundamental Algorithms for Scientific Computing in Python. *Nature Methods* 17, 261–272. <https://doi.org/10.1038/s41592-019-0686-2>

Wachholz, A., Jawitz, J.W., Büttner, O., Jomaa, S., Merz, R., Yang, S., Borchardt, D., 2022. Drivers of multi-decadal nitrate
865 regime shifts in a large European catchment. *Environ. Res. Lett.* 17, 064039. <https://doi.org/10.1088/1748-9326/ac6f6a>

Formatiert: Deutsch (Deutschland)

Wachholz, A., Borchardt, D., 2024. Vom Eisernen Vorhang zum grünen Band 2024. *Korrespondenz Wasserwirtschaft*. 04/24,
245–251. <https://doi.org/10.3243/kwe2024.04.002>

Formatiert: Deutsch (Deutschland)

Formatiert: Deutsch (Deutschland)

Formatiert: Deutsch (Deutschland)

870 Wang, J., Xia, X., Liu, S., Zhang, S., Zhang, L., Jiang, C., Zhang, Z., Xin, Y., Chen, X., Huang, J., Bao, J., McDowell, W.H.,
Michalski, G., Yang, Z., Xia, J., 2022. The Dominant Role of the Water Column in Nitrogen Removal and N₂O Emissions
in Large Rivers. *Geophysical Research Letters* 49. <https://doi.org/10.1029/2022GL098955>

Feldfunktion geändert

Wanninkhof, R., 1992. Relationship between wind speed and gas exchange over the ocean. *Journal of Geophysical Research: Oceans* 97, 7373–7382. <https://doi.org/10.1029/92JC00188>

Weiss, R.F., 1970. The solubility of nitrogen, oxygen and argon in water and seawater. *Deep Sea Research and Oceanographic Abstracts* 17, 721–735. [https://doi.org/10.1016/0011-7471\(70\)90037-9](https://doi.org/10.1016/0011-7471(70)90037-9)

880 Westphal, K., Graeber, D., Musolff, A., Fang, Y., Jawitz, J.W., Borchardt, D., 2019. Multi-decadal trajectories of phosphorus loading, export, and instream retention along a catchment gradient. *Science of The Total Environment* 667, 769–779. <https://doi.org/10.1016/j.scitotenv.2019.02.428>

Formatiert: Deutsch (Deutschland)

Zhang, X., Yang, X., Hensley, R., Lorke, A., Rode, M., 2023. Disentangling In-Stream Nitrate Uptake Pathways Based on Two-Station High-Frequency Monitoring in High-Order Streams. *Water Resources Research* 59, e2022WR032329. <https://doi.org/10.1029/2022WR032329>

Formatiert: Deutsch (Deutschland)

Zill, J., Siebert, C., Rödiger, T., Schmidt, A., Gilfedder, B.S., Frei, S., Schubert, M., Weitere, M., Mallast, U., 2023. A way to determine groundwater contributions to large river systems: The Elbe River during drought conditions. *Journal of Hydrology: Regional Studies* 50, 101595. <https://doi.org/10.1016/j.ejrh.2023.101595>

890